



Classification of EEG Mental Tasks using Multi-Objective Flower Pollination Algorithm for Person Identification

Zaid Abdi Alkareem Alyasseri^{1,2,*}, Ahamad Tajudin Khader¹, Mohammed Azmi Al-Betar³, Joao P. Papa⁴, Osama Ahmad Alomari¹, Sharif Naser Makhadmeh¹

¹School of Computer Sciences,
Universiti Sains Malaysia, Pulau Pinang, Malaysia.

²ECE Department-Faculty of Engineering,
University of Kufa, Najaf, Iraq

³Depart. of information technology,
Al-Huson University College, Al-Balqa Applied University, Al-Huson, Irbid, Jordan.

⁴ Department of Computing,
San Paulo State University, Bauru, Brazil.

*Corresponding Author

DOI: <https://doi.org/10.30880/ijie.2018.10.07.010>

Received 8 September 2018; Accepted 19 November 2018; Available online 30 November 2018

Abstract: In the modern life, the authentication technique for any system is considered as one of the most important challenges task which must careful consideration. Therefore, many researchers have developed traditional authentication systems to deal with our digital world. Recently, The Biometric techniques have been successfully provided a high level of authentication, such as fingerprint, face recognition, and voice recognition. In this paper, a new authentication system has been proposed which is based on EEG signals with hybridizing wavelet transform and multi-objective flower pollination algorithm (MOFPA-WT). The main task of MOFPA is to find the optimal WT parameters for EEG signal denoising which can extract unique features form the EEG. The proposed method (MOFPA-WT) tested using a standard EEG database which has five different mental tasks, includes baseline, multiplication, rotation, letter composing, and visual counting. To classify the EEG signals using proposed method four classification methods are applied which are, neural network, decision tree, Naive Bayes, and support vector machine. The performance of the (MOFPA-WT) is evaluated using four criteria: (i) accuracy, (ii) sensitivity, (iii) specificity, (v) false acceptance rate. The experimental results show the (MOFPA-WT) can achieve the highest recognition rates up to 85% using neural network classifier based on visual counting task as well as the EEG_std feature obtained the highest accuracy compared with others EEG features based on visual counting task.

Keywords: EEG, Wavelet, Signal decomposition, Flower pollination algorithm, Multi-Objective, Identification.

1. Introduction

Electroencephalogram (EEG) is a graphical recording of brain electrical activity that is recorded from the scalp. This recording represents the voltage fluctuations resulting from ionic current flows within the neurons of the brain (Abdulkader et. al, 2015). Therefore, EEG signals can provide most of the required information about brain activity. EEG signals from the brain are captured using **invasive** or **non-invasive** techniques (Abdulkader et. al, 2015; Ramadan &

Vasilakos, 2017). The main difference between these techniques is that the invasive approach involves the use of electrode arrays implanted inside the brain, such as **ECoG BCI** for arm movement control (Rao, 2013). Meanwhile, there are several techniques to record the brain activity can also be captured using different types of signal capturing devices, including EEG for electrical activity from the scalp, MEG for magnetic field fluctuations caused by electrical activity in the brain, and fMRI and fNIR for changes in blood oxygenation level resulting from neural activity (Abdulkader et. al, 2015; Ramadan & Vasilakos, 2017).

In (Berger, 1929), Hans Berger proposed for the first time the use of EEG signals as a non-invasive technique for capturing brain activities. Over the past several decades, researchers have developed Hans's technique to suit multiple applications. For instance, EEG signals have been used in medical applications for prevention, detection diagnosis, rehabilitation and restoration of patient. This technique has also been used for non-medical applications, such as education and self-regulation, neuromarketing and advertisement, neuroergonomics and smart environment, games and entertainment, and learning and education as summarized in (Ramadan & Vasilakos, 2017). Recently, EEG signals have been successfully used as a new biometric technique in security and authentication applications (Kumari & Vaish, 2015; Kumari & Vaish, 2016; Ramadan & Vasilakos, 2017).

Pinki Kumar et. al. in (Kumari & Vaish, 2015) proposed a user identification system based on EEG signal collected from six users using EMOTIVE EPOC headset which has 14 channels. In feature extraction phase, wavelet transform (WT) technique is proposed to extract the unique features of EEG signal. In addition, three basic statistical measurements extracted from EEG signal includes Mean, Standard deviation, and Energy for each sub-band rhythm. Later, same authors investigated some cognitive tasks for individual identification system (Kumari & Vaish, 2016). They used standard EEG datasets which are motor/movement and imaginary (Schalk et. al, 2004) where they used one channel (i. e. Cz) to get the input EEG signal. In addition, they also used WT to decompose the EEG signal into 5 level to extract four different features from each sub-band which are namely: Energy, Logarithm energy, Absolute energy, and REE energy. Ferdous Jannatul in (Ferdous, 2016) proposed a biometric method using the power spectral density (PSD) estimates of EEG over the combined Alpha-Beta rhythm of the EEG signal. The authors tested the proposed method on using ANT Neuro device for capture the EEG signals from two persons. Finally, the author obtains classification accuracy equal 50%. Zahhad et. al. in (Abo-Zahhad et. al, 2016) introduced a new method to improve the performance of the EEG based biometric authentication using eye blinking EOG signals which are considered as source of artifacts for EEG. Rodrigues et. al. in (Rodrigues et. Al, 2016) used binary flower pollination algorithm (Yang, 2013; Yang et. al, 2014) to obtain the best channel which can provide the highest recognition rate for person identification based on EEG signal. Their work was tested using a standard EEG datasets which are motor / movement and imaginary. Finally, their work able to obtain the highest recognition rate equal (87%) with reducing the number of EEG channels to half. Table 1 shows the comparative analysis of EEG-based authentication system.

Table 1 – Comparative analysis of EEG-based authentication system.

Ref.	Year	Dataset	Features Extraction	Classifier	Performance
Pinki Kumar et al (Kumari & Vaish, 2015)	2015	Self-collected	Mean, Std, and Energy	LVQ-NN	Sensitivity=0.95%
Pinki Kumar et al (Kumari & Vaish, 2016)	2016	motor/movement and imaginary	Energy, Logarithm energy, Absolute energy, and REE energy	Neural Network (NN)	TAR =94.28% FRR =0.5%
Ferdous Jannatul in (Ferdous, 2016)	2016	Self-collected	PSD over Alpha-Beta rhythm	Euclidean distance	ACC=50%
Zahhad et. al. in (Abo- Zahhad et. al, 2016)	2016	Self-collected	Auto-Regressive	linear discriminant analysis (LDA)	EERs of 0.89%
Rodrigues et. al. in (Rodrigues, Silva, Papa, Marana, & Yang, 2016)	2016	motor/movement and imaginary	Auto-Regressive	OPF	ACC=87%

The main objective of this paper is to propose a multi-objective flower pollination algorithm with wavelet transform (MOFPA-WT) to decompose the input EEG signal to find the optimal features which can achieve the highest accuracy. MOFPA-WT applied using two objective functions which are: $\min(MSE)$ and $\max(SNR)$ to obtain the best combination of WT parameters for EEG signal denoising. The proposed method is implemented according to the weighted sum approach to combine multi-objectives into a composite one objective function. The original EEG signal is taken from a standard EEG dataset which is *Keirn* EEG dataset which has five different mental tasks, includes baseline, multiplication two numbers, geometric figure rotation, letter composing, and visual counting each task repeated several times for ten seconds and the EEG signals collected from seven subjects (Keirn & Aunon, 1990). The original EEG signals decompose into five level to extract the unique features from each sub-band (i.e. high gamma, gamma, alpha, beta, theta, and delta) where four features are extracted which are namely: mean, standard deviation, entropy, and energy. For evaluating the performance of MOFPA-WT, the results are evaluated in terms of four factors: accuracy rate, sensitivity, specificity, and

false acceptance rate (FAR). It is worth mentioning that the proposed method achieves the highest accuracy result which can be obtained using mental tasks based on visual counting compared with mental tasks.

This paper is organized as follows. Section 2 describes a wavelet transform and the principal of WT for EEG signal denoising. Section 3 provides a background about the flower pollination algorithm and its multi-objective technique. Section 4 describes the proposed system. The results and discussion describe in section 5. Finally, the conclusion and future works describe in section 6.

2. EEG Signal Denoising using Wavelet Transform

Wavelet Transform (WT) is a powerful and common tool for time-frequency domain signal representation. WT has successfully applied for signal compression, feature extraction and selection, and others (Alyasseri et. al, 2017a; Alyasseri et. al, 2017b; Alyasseri et. al, 2017c; Alyasseri et. al, 2018). In general, the WT can be classified into two types: discrete wavelet transform (DWT) and continuous wavelet transform (CWT). In the recent few years, the WT has been extensively used with non-stationary signals, such as ECG and EEG because the WT has shown powerful outcomes in removing several EEG artifact noises and extracting the EEG features (Alyasseri et. al, 2017). In this paper, the DWT has been used to decompose the input EEG signal to extract unique features from each EEG sub-bands (i.e., high gamma, gamma, alpha, beta, theta, and delta). One of the popular methods for DWT is proposed in (Donoho & Johnstone, 1994) and so-called Donoho’s approach which extracted as follows:

$$C(a, b) = \sum_{n \in \mathbb{Z}} x(n)g_{j,k}(n) \quad (1)$$

where $C(a,b)$ denotes the wavelet dynamic coefficients, $a = 2^{-j}$, $b = k2^{-j}$, $j \in \mathbb{Z}$, $k \in \mathbb{Z}$; a is the size of the time scale, b is the translation, $x(n)$ is the input EEG signal, and $g_{j,k}(n) = 2^{j/2} g(2^j n - k)$ is the DWT.

The task of DWT is to decompose the input signal using different coefficients levels to correct the high frequency of the input signal. The denoising process involves three phases:

- 1- **EEG signal decomposition**, the original EEG signal will be divided into five levels, at each level the EEG signal will be decomposed into two parts namely Approximation coefficients (cA), and Detail coefficients (cD). The cD will process using high-pass filter and cA will be continuously decomposed for next level.
- 2- **Thresholding** where for each level a threshold value defined according to the coefficients noise level.
- 3- **Reconstruction**, the EEG denoised signal is reconstructed using inverse discrete wavelet transform iDWT.

The WT has five parameters where each parameter has different types (See Table 2). The efficiency of noise reduction and unique features extraction relies on the selection of wavelet parameters. The wavelet denoising process has three phases: The first phase is the decomposition of the EEG signal using DWT. This phase involves selecting the appropriate mother wavelet function (Φ) for use in the EEG signal decomposition task. The second wavelet parameter, that is, the decomposition level (L), is also selected in this phase normally based on the EEG signal and experience. It should be noted that the selection of appreciating parameters of WT (which is one of the main goal of this paper) is recently accomplished using optimization techniques such FPA, β -hill climbing (β -hc), and genetic algorithm (GA) (Alyasseri et. al, 2017; Alyasseri et. al, 2017).

In the second phase, thresholding is applied. The wavelet provides two standard types of thresholding functions (β), namely, hard and soft thresholding (Donoho & Johnstone, 1994). The thresholding type (soft or hard), selection rules (λ), and rescaling methods (ρ) must all be selected. These threshold mechanisms must be applied because the selection will affect the global denoising performance. The thresholding value is generally defined based on the standard deviation (σ) of the noise amplitude. The wavelet parameters (β , λ , and ρ) must be separately applied for each wavelet coefficient (cA and cD) level. In the last phase, the denoised EEG signal is reconstructed by iDWT.

Table 2. Wavelet Parameters Range

Wavelet parameters	Range
Mother wavelet (Φ)	Daubechies (db2..db45), Symlet (sym1..45), Coiflet (coif1..coif5), and Biorthogonal (bior1.1..bior3.9)
Decomposition level (L)	5
Thresholding type (β)	soft and hard
Selection method (λ)	Heursure, Rigrsure, Sqtwolog, and Minimax
Rescaling approach (ρ)	sln, one, and mln

3. Background

This section provides a background about the flower pollination algorithm and its multi-objective version. Section 3.1 introduces the flower pollination algorithm. Section 3.2 explains the concepts of the multi-objective optimization.

3.1 Flower Pollination Algorithm

In the recent optimization review, the meta-heuristic algorithms can be classified into evolutionary algorithm (Al-Betar et al. 2016 ; Alyasseri et al. 2012), swarm intelligence (Alyasseri et al. 2018), and trajectory algorithms (Abualigah et al. 2017; Al-Betar & Azmi, 2017).

Flower pollination algorithm (FPA) is one of successful swarm-based intelligence which is inspired from the pollination behavior of the flowering plants. FPA is introduced by Yang in 2012 (Yang, 2013; Yang et al. 2014) and successfully applied for many optimization problems (Abdi et al., 2018; Rodrigues et al. 2016).

The rules (operators) of FPA are summarized as follows:

Rule (1): Global pollination involves the biotic and cross-pollination where the pollinators are carrying the pollen-based on Levy flights.

Rule (2): Local pollination involves abiotic and self-pollination.

Rule (3): The reproduction probability can be considered as the flower constancy is proportional to the similarity between any two flowers.

Rule (4): The switch probability $p \in [0; 1]$ can be controlled between local pollination and global pollination

Due to some external factors such as wind, local pollination will be a significant fraction p in the overall pollination activities. Figure 1 shows the flowchart of flower pollination algorithm.

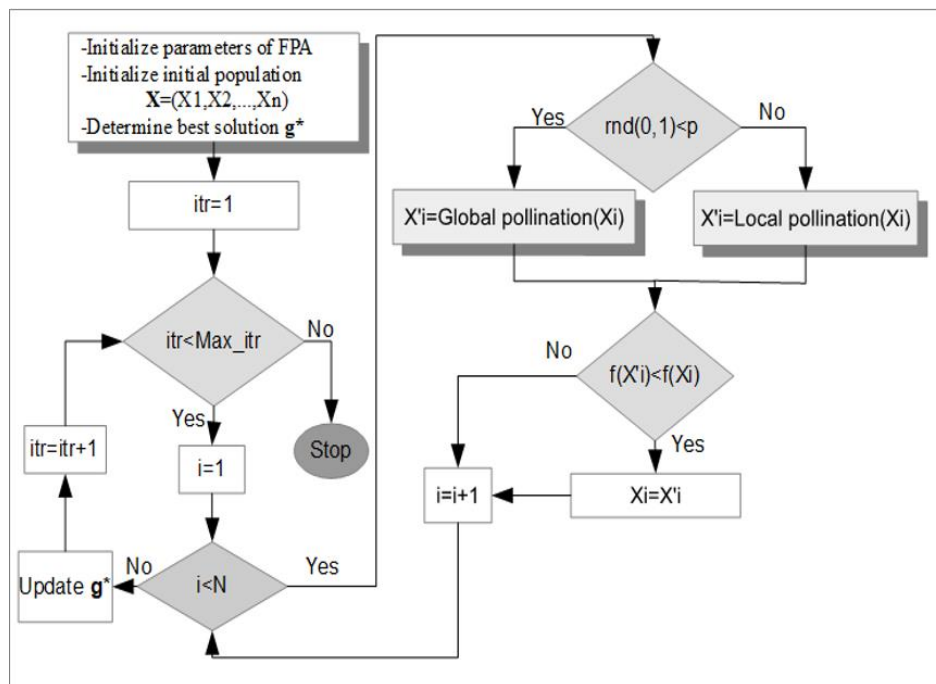


Figure 1: FPA Flowchart

3.2 Multi-objective optimization

This section describes a briefly introduction about multi-objective optimization technique. In general, the multi-objective optimization refers to solve any optimization problem using more than one objective function (Yang et al. 2014). The multi-objective optimization problem for n objectives functions can be formulated as follows:

$$\text{Minimize } F(x) = f_1(x), f_2(x), \dots, f_n(x) \quad (2)$$

where n refers to number of objective functions.

The FPA has been extended to multi-objective optimization technique by Yang et al. (Yang et al. 2014), while the author adapted multi-objective flower pollination algorithm (MOFPA) for solving engineering optimization problems. MOFPA is implemented according to the weighted sum approach to combine two objectives into a composite one objective function.

4. Proposed Work

This section provides a discussion for the proposed system for EEG signals-based user authentication. The proposed system run through four phases where the result of each phase is an input to the consecutive one. Phase 1 EEG signal

acquisition describes in Section 4.1. Section 4.2 describes Phase 2 Tuning WT parameters by using MOFPA using hybridizing between multi-objective flower pollination algorithm with wavelet transform (MOFPA-WT). Phase 3 Feature extraction from denoised EEG signals presents in Section 4.3. Phase 4 EEG signal classification using neural network classifier presents in Section 4.4. The four phases are flowcharted in Figure 2 and thoroughly are described as follows:

4.1 EEG signal acquisition

In this study, Keirn EEG dataset has been used. More details about this dataset given in Section 5. Where the original EEG signal processed using a Butterworth 5th order filter with range 6-30Hz to achieve the highest signal-to-noise ratio (SNR) and obtained the efficient features extraction.

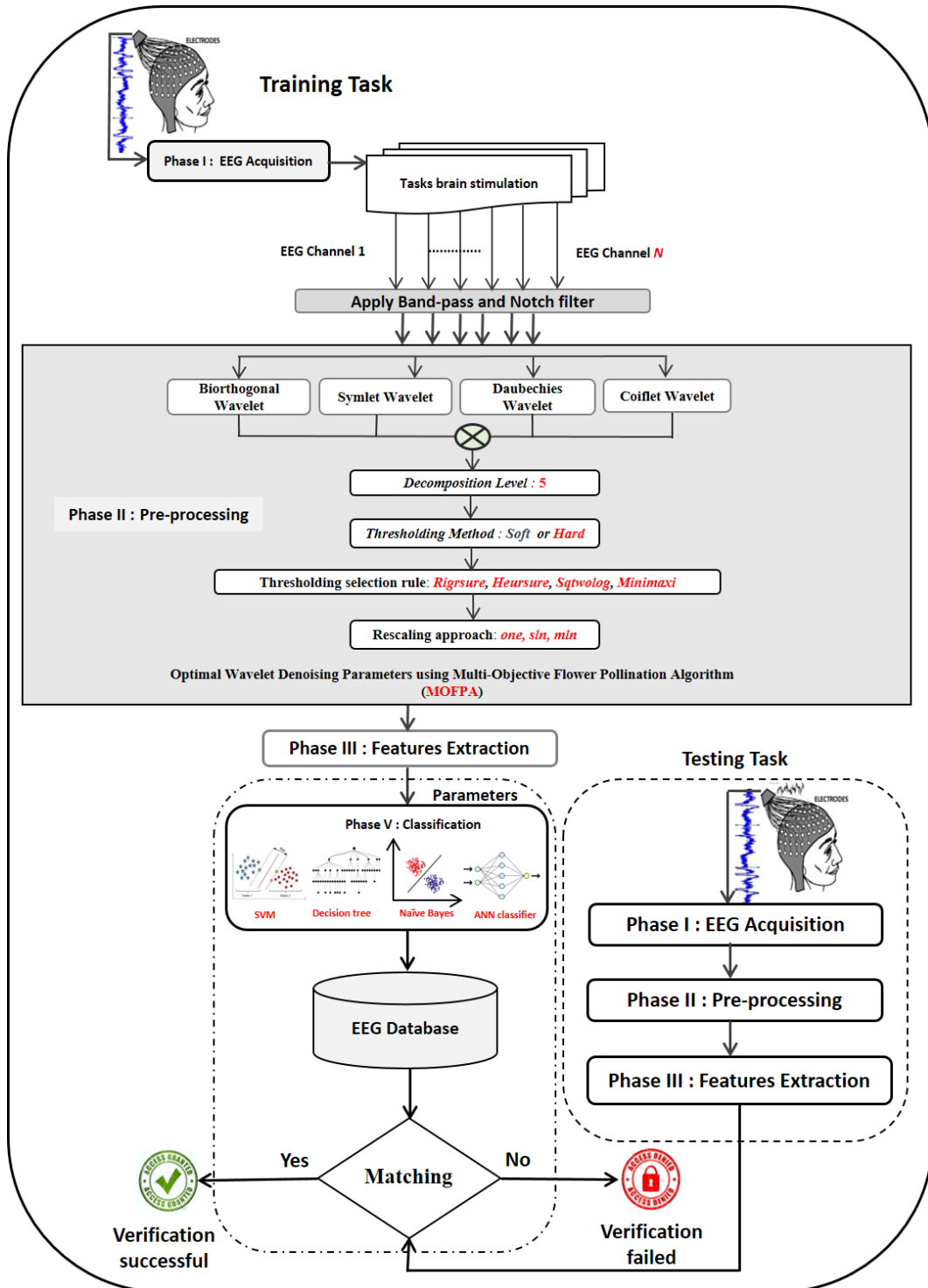


Figure 2: Proposed system flowchart

4.2 EEG signal denoising using MOFPA-WT

In this paper, we propose to estimate the optimum/near-optimum set of parameters concerning the Wavelet Transform for EEG signal denoising as a multi-objective optimization task. In our approach, the set of WT parameters is represented as a vector $x=(x_1, x_2, \dots, x_d)$ where d is the number of parameters used for the Wavelet Transform (In this paper, $d=5$). In this context, x_1 represents the value of the mother wavelet function parameter, x_2 stands for the value of the decomposition level parameter, x_3 refers to the thresholding method, x_4 represents the value of the thresholding selection rule parameter, and x_5 represents the re-scaling approach.

The proposed MOFPA-WT evaluates each solution using the multi-objective framework applying two objective functions: $\min(\text{MSE})$ and $\max(\text{SNR})$, as formulated below:

$$F_{\text{MOFPAWT}} = W_1 f_1 + W_2 f_2, \tag{3}$$

$$F_{\text{MOFPAWT}} = W_1 * \min(\text{MSE}) + W_2 * \max(\text{SNR})$$

where the weight vector is initialized as follows: W_1 is rand between (0,1) and $W_2=1-W_1$.

The two objective functions which are mean squared error (MSE) and signal-to-noise ratio (SNR) are formulated as below:

$$\text{MSE} = \frac{1}{N} \sum_{i=1}^N (x(i) - \hat{x}(i))^2, \tag{4}$$

And

$$\text{SNR} = 10 \log_{10} \left\{ \frac{\sum_{i=1}^N [x(i)]^2}{\sum_{i=1}^N [x(i) - \hat{x}(i)]^2} \right\} \tag{5}$$

where $x(i)$ and $\hat{x}(i)$ denote the original and denoised EEG signals, respectively. Notice that $\hat{x}(i)$ is obtained using the Wavelet Transform tuned by the proposed MOFPA-WT.

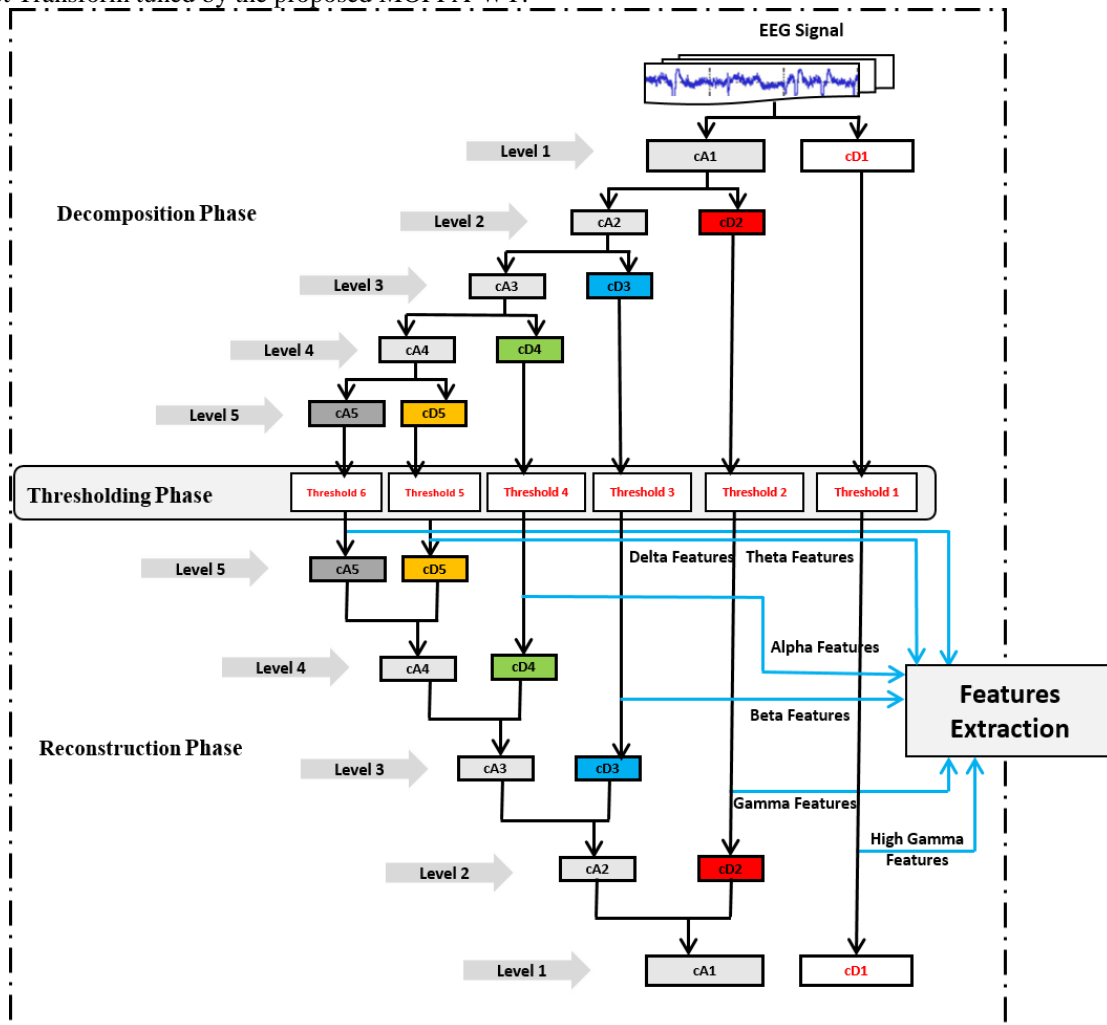


Figure 3: EEG feature extraction based on WT 5 decomposition level

Iteratively, the randomly generated solutions undergo refinement using the MOFPA-WT. The result of this phase is an optimized solution that will be passed to the denoising phase, which involves three main steps that are depicted in Figure 4 and described in more details below:

1. **EEG signal decomposition using DWT:** in this step, the DWT is applied to decompose the noise of the input EEG signals. In such process, one uses the first two optimal parameters (i.e., the mother WT function and the decomposition level) only. Figure 4 shows the DWT procedure for 5 levels, where the EEG signal is partitioned at each level into cA and cD components. The latter is processed using a high-pass filter, while the former is processed using a low-pass filter and is decomposed for the next level.
2. **Thresholding:** it is applied based on the noise level of the coefficients. In this step, the last three wavelet parameters, namely, the thresholding type, the thresholding selection rules, and the re-scaling methods, must be selected from optimal parameters which are obtained based MOFPA-WT.
3. **Reconstruction of the denoised EEG signal by iDWT:** we estimate the value of the original EEG signals by applying iDWT on their denoised version. The reconstruction convolves the EEG data using up sampling, which involves the addition of zeros at the even index elements of the signal.

4.3 Feature Extraction

Extracting efficient features considers a significant phase in any authentication system because it will increase the performance of the proposed system to get good results in the correct classification. Therefore, the main purpose of this phase is to find the unique characteristics features from each sub-band (i.e., high gamma, gamma, alpha, beta, theta, and delta). Figure 3 shows feature extraction-based WT decomposition with five levels. There are several features that can be extracted from the denoised EEG signal. In this paper, we applied we have used four popular measurements of the signal which are **mean**, **standard deviation**, **entropy**, and **energy** where these features are able to provide a unique pattern among the users. These four features are formulated as follows:

$$EEG_{mean} = \frac{1}{N} * \sum_{j=1}^N D_{ij}, \quad i = 1,2,3, \dots, L \quad (6)$$

$$EEG_{std} = \sqrt{\frac{1}{N} * \sum_{j=1}^N (x_j - \hat{x})^2} \quad i = 1,2,3, \dots, L \quad (7)$$

$$EEG_{Energy} = \sum_{j=1}^M |D_{ij}|^2, \quad i = 1,2,3, \dots, L \quad (8)$$

$$EEG_{Entropy} = - \sum p(x) \log p(x), \quad (9)$$

4.4 Classification

To classify the extracted features from the denoised EEG signal into correct person four popular classifiers have been applied which are: artificial neural network (NN), Naïve Bayes, Decision Tree (J48), and support vector machine (SVM). We used Weka tool for classification task and designed a network with 24-input features vector of each subject (i. e., 4 features * 6 sub-bands). Table shows the classifiers configuration which are used in this paper.

Table 3 –Classifiers configuration.

Classifier	Hidden layer	Learning Rate	Binary Splits	Test mode
NN	32	0.3	yes	10-fold cross-validation
Classifier	C	Gamma	Kernel	Test mode
SVM	1.0	1.0E-12	polynomial	10-fold cross-validation
Classifier	C	Gamma	Binary Splits	Test mode
Naïve Bayes	0.691	0.95	yes	10-fold cross-validation
Classifier	Confidence Factor	seed	Binary Splits	Test mode
Decision Tree (J48)	0.25	1	False	10-fold cross-validation

5. Results and Discussion

Keirn EEG dataset has been used in this paper. This dataset recorded EEG from seven subjects while they were performing different mental tasks exploring new human-machine interaction through the brain (Alyasseri et. al, 2018). Although a small database (7 subjects: males and females between the ages of 21 and 48) the relevance of this database resides on the multi-task recording paradigm. A total of 5 tasks were performed by subjects. Each task was repeated 5 times and recorded under both Rest Eyes Closed (REC) and Rest Eyes Open (REO) on every session. This EEG dataset was recorded with samples rate at 250 Hz for 10 seconds, seconds for each task, that means total EEG signal size is 2500

samples. Furthermore, this dataset has only six channels which are namely: C3, C4, P3, P4, O3, and O4. The recording tasks of this dataset as follows:

Task 1 **Baseline** measurements. This task was taken as a baseline for comparison. In this case, subjects were only asked to relax.

Task 2 **Complex problem-solving**. Subjects were asked to mentally solve non-trivial multiplication problems.

Task 3 **Geometric figure rotation**. Subjects were presented with an image of a 3-dimensional complex object before being asked to mentally rotate it.

Task 4 **Mental letter composition**. Subjects had to mentally write a letter to a friend or a family member.

Task 5 **Visual counting**. Subjects were asked to visualize numbers being written on a blackboard sequentially.

With the previous number being erased before a new number is written. Figure 4 shows the distribution of electrodes in Keirn's EEG dataset with six channels

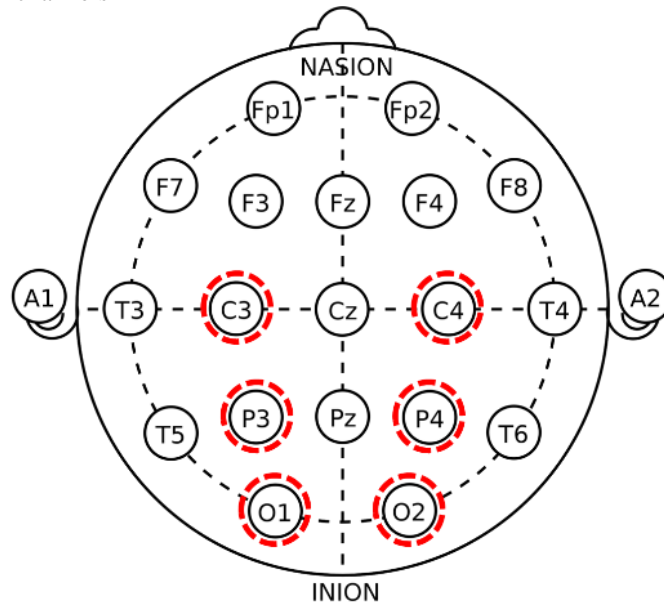


Figure 4: Distribution of electrodes in Keirn's EEG dataset

The EEG dataset which used in this paper has been separated into five different mental tasks based on 10folds cross-validation technique for training and testing for each task. To evaluate the performance of the MOFPA-WT method four measures have been calculated namely, accuracy, sensitivity, specificity, false acceptance rate which can be formulated as follows:

$$\text{Accuracy} = \frac{TA + TR}{TA + FA + TR + FR} * 100 \quad (10)$$

$$\text{Sensitivity}(TAR) = \frac{TA}{TA + FR} \quad (11)$$

$$\text{Specifity}(TFR) = \frac{TR}{TR + FR} \quad (12)$$

$$FAR = 1 - TFR \quad (13)$$

where TA, TR, FA, and FR represent the true acceptance, true reject, false acceptance, and false reject, respectively. The results of the classification phase are represented as a confusion matrix that tabulates whether they fall into one of four categories: TA, TR, FA and FR.

Figure 5 shows the accuracy rate considering the input EEG signals based on five decomposition levels using MOFPA-WT. For the sake of visualization purposes, this chart summarizes the experiments conducted in this work. One can observe that the multi-objective paradigm is quite promising to be applied in the context of EEG signal denoising based on the Wavelet Transform. The results obtained are pretty much interesting and they can be extended to larger datasets when they happen to be available. With such a combined framework, we can learn, simultaneously, how to reconstruct and denoise the signal.

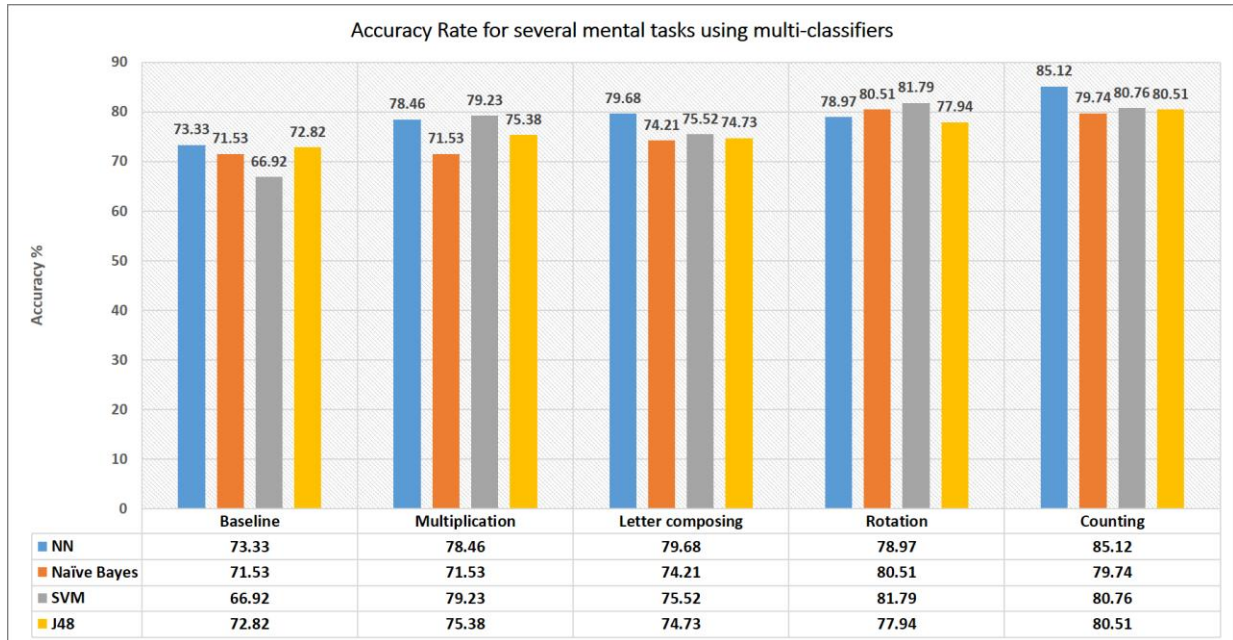


Figure 5 – Accuracy rate using different mental tasks.

where TA, TR, FA, and FR represent true acceptance, true reject, false acceptance, and false reject, respectively. The results of classification, phase is represented as a confusion matrix that tabulates whether they fall into one of four categories: true acceptance (TA), true reject (TR), false acceptance (FA) and false reject (FR). Tables (4-8) show the confusion matrixes according to baseline, multiplication, letter composition, rotation, and counting task, respectively. Overall, subject seven obtains the best results during the test for all tasks where it achieved the highest sensitivity value=1 with counting task using NN and SVM classifier. The highest accuracy is obtained with counting task, while the accuracy=85.12%, and FAR= 14.87% using NN classifier. Figure 5 shows the accuracy rate for the input EEG signals based on five decomposition level using MOFPA-WT for baseline, multiplication, rotation, letter composition, and counting task, respectively based on several classifiers methods which are artificial neural network (NN), Naïve Bayes, Decision Tree (J48), and support victor machine (SVM). Figure 6 shows the FAR using several classifiers method, while the best results has been achieved with NN classifiers. Table 9 show a comparison based on EEG features extraction using neural network (NN) classifier. The results show that the EEG_{Std} provided the highest accuracy rate with 84% correction rate compared with others features, where these features achieved.

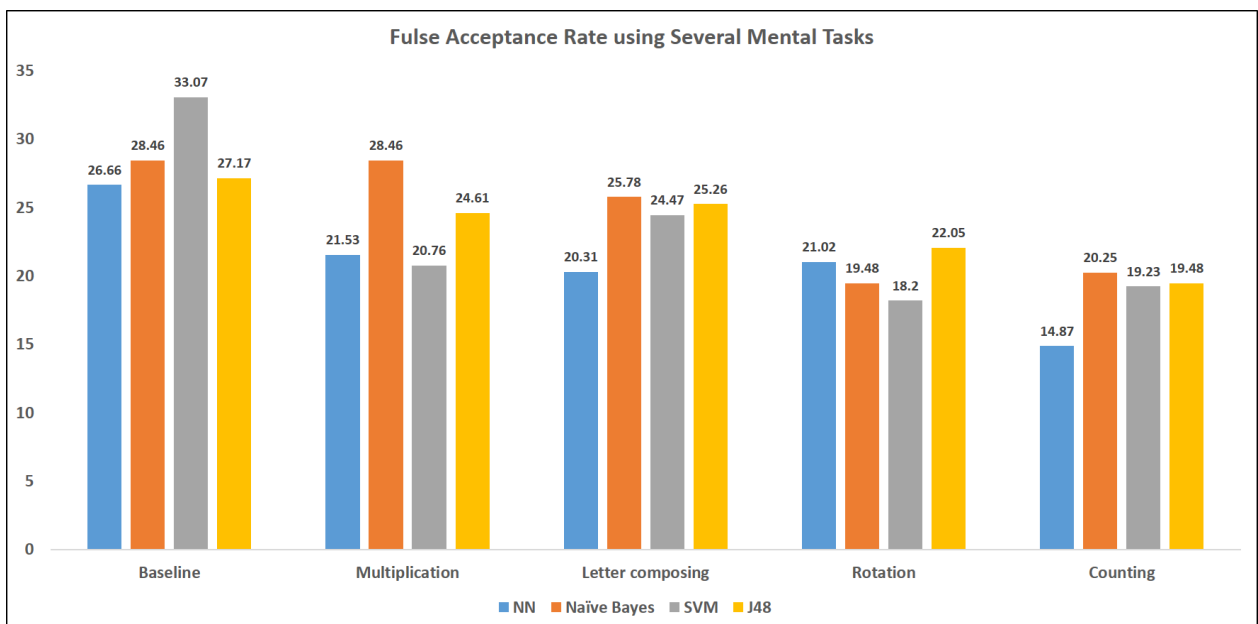


Figure 6– False acceptance rate using different mental tasks.

6. Conclusions and future work

In this paper, a novel technique for EEG signal denoising based on multi-objective flower pollination algorithm with wavelet transform (MOFPA-WT) is proposed. The main task of MOFPA-WT method is to find the efficient decomposition of the input EEG signal which can provide unique features from each sub-band. MOFPA-WT is tested using a standard EEG signal dataset, namely, Keirn EEG dataset which have five mental tasks includes base line, multiplication, rotation, letter composition, and counting task, respectively. The performance of MOFPA-WT is evaluated using four criteria: accuracy, sensitivity, specificity, and false acceptance rate.

In conclusion, the proposed method achieves the highest accuracy result which can be obtained using mental tasks based on visual counting task compared with mental tasks. Also, the proposed method shows that the brainwave signal provided unique features which can be used as new biometric technique.

For future work, MOFPA-WT will be applied for more challenging signal problem instances, such as user authentication with large EEG dataset or early detection of epilepsy based on EEG signal. Furthermore, the real-world applications are required to show the efficiency of MOFPA-WT. Other possible improvements are applying one of features selection technique is recommended to increase the accuracy rate as well as to reduce the dimensions redundancy of the extracted. Regarding future works, we intend to apply MOFPA-WT in more challenging signal problem instances, such as user authentication or early detection of epilepsy based on EEG signals, as well as to consider MOFPA-WT in larger datasets for EEG-based person identification.

Table 4 - Baseline task results.

NN	Person1	Person2	Person3	Person4	Person5	Person6	Person7	Sensitivity	Specificity	FAR	ACC
Person1	49	0	0	10	0	0	1	0.817	0.942	0.183	92.3
Person2	0	19	1	2	0	8	0	0.633	0.977	0.367	95.1
Person3	1	2	47	1	1	6	2	0.783	0.975	0.217	94.6
Person4	15	1	1	34	3	0	6	0.567	0.924	0.433	86.9
Person5	0	1	0	6	78	5	0	0.867	0.95	0.133	93
Person6	0	4	5	1	10	40	0	0.667	0.939	0.333	89.7
Person7	3	0	1	5	1	1	19	0.633	0.975	0.367	94.8
Naïve Bayes	Person1	Person2	Person3	Person4	Person5	Person6	Person7	Sensitivity	Specificity	FAR	ACC
Person1	51	0	0	7	0	0	2	0.85	0.966	0.15	94.9
Person2	0	23	3	0	2	2	0	0.767	0.958	0.233	94.4
Person3	0	2	49	1	0	6	2	0.817	0.96	0.183	93.8
Person4	10	1	2	28	4	0	15	0.467	0.927	0.533	85.6
Person5	0	1	0	13	73	0	3	0.811	0.94	0.189	91
Person6	0	11	6	0	9	34	0	0.567	0.975	0.433	91.3
Person7	1	0	2	3	3	0	21	0.7	0.938	0.3	92.1
Decision Tree	Person1	Person2	Person3	Person4	Person5	Person6	Person7	Sensitivity	Specificity	FAR	ACC
Person1	46	0	0	11	0	0	3	0.767	0.981	0.233	94.9
Person2	0	17	1	2	4	6	0	0.567	0.963	0.433	93.3
Person3	0	5	47	2	1	3	2	0.783	0.969	0.217	94.1
Person4	4	3	3	39	4	0	7	0.65	0.918	0.35	87.7
Person5	0	1	2	5	75	7	0	0.833	0.926	0.167	90.5
Person6	0	4	3	0	10	43	0	0.717	0.951	0.283	91.5
Person7	2	0	1	7	3	0	17	0.567	0.966	0.433	93.6
SVM	Person1	Person2	Person3	Person4	Person5	Person6	Person7	Sensitivity	Specificity	FAR	ACC
Person1	54	0	0	6	0	0	0	0.9	0.9	0.1	90
Person2	0	3	1	4	3	19	0	0.1	0.997	0.9	92.8
Person3	0	0	51	2	0	7	0	0.85	0.954	0.15	93.8
Person4	23	0	2	31	4	0	0	0.517	0.912	0.483	85.1
Person5	1	1	0	3	85	0	0	0.944	0.916	0.056	92.3
Person6	0	0	8	0	15	37	0	0.617	0.921	0.383	87.4
Person7	9	0	4	14	3	0	0	0	1	1	92.3

Table 5 – Multiplication task results.

NN	Person1	Person2	Person3	Person4	Person5	Person6	Person7	Sensitivity	Specificity	FAR	ACC
Person1	49	0	0	6	0	0	5	0.817	0.951	0.183	93.1
Person2	0	22	1	2	0	5	0	0.733	0.969	0.267	95.1
Person3	0	2	53	0	1	1	3	0.883	0.987	0.117	97.2
Person4	7	0	1	37	13	2	0	0.617	0.942	0.383	89.2
Person5	0	0	0	10	78	2	0	0.867	0.946	0.133	92.8
Person6	0	9	0	0	2	49	0	0.817	0.969	0.183	94.6
Person7	9	0	2	1	0	0	18	0.6	0.977	0.4	94.9
Naive Bayes	Person1	Person2	Person3	Person4	Person5	Person6	Person7	Sensitivity	Specificity	FAR	ACC
Person1	49	0	0	7	0	0	4	0.817	0.951	0.183	93.1
Person2	0	22	0	1	1	5	1	0.733	0.947	0.267	93.1
Person3	0	8	34	0	0	11	7	0.567	0.987	0.433	92.3
Person4	8	1	0	32	18	1	0	0.533	0.951	0.467	88.7
Person5	2	0	2	4	79	1	2	0.878	0.92	0.122	91
Person6	0	10	1	3	5	41	0	0.683	0.945	0.327	90.5
Person7	6	0	1	1	0	0	22	0.733	0.961	0.267	94.4
Decision Tree	Person1	Person2	Person3	Person4	Person5	Person6	Person7	Sensitivity	Specificity	FAR	ACC
Person1	49	0	0	7	0	0	4	0.817	0.951	0.183	93.1
Person2	0	18	1	1	0	9	1	0.6	0.958	0.4	93.1
Person3	0	2	54	0	0	1	3	0.9	0.981	0.1	96.9
Person4	8	0	1	36	15	0	0	0.6	0.936	0.4	88.5
Person5	0	0	0	11	77	2	0	0.856	0.94	0.144	92.1
Person6	0	10	1	1	3	45	0	0.75	0.963	0.25	93.1
Person7	8	3	3	1	0	0	15	0.5	0.977	0.5	94.1
SVM	Person1	Person2	Person3	Person4	Person5	Person6	Person7	Sensitivity	Specificity	FAR	ACC
Person1	51	0	0	5	2	0	2	0.85	0.96	0.15	94.4
Person2	0	14	5	0	2	8	1	0.467	0.969	0.533	93.1
Person3	0	5	52	0	0	0	3	0.867	0.978	0.133	96.2
Person4	4	1	0	39	15	1	0	0.65	0.975	0.35	92.6
Person5	0	0	0	3	86	1	0	0.956	0.913	0.044	92.3
Person6	0	4	0	0	7	49	0	0.817	0.969	0.183	94.6
Person7	9	1	2	0	0	0	18	0.6	0.983	0.4	95.4

Table 6 – Letter Composing task.

NN	Person1	Person2	Person3	Person4	Person5	Person6	Person7	Sensitivity	Specificity	FAR	ACC
Person1	56	0	0	1	0	0	3	0.933	0.975	0.067	96.9
Person2	1	21	0	3	2	3	0	0.7	0.968	0.3	94.8
Person3	0	0	56	1	0	2	1	0.933	0.978	0.067	97.1
Person4	3	2	1	37	5	3	3	0.685	0.945	0.315	90.9
Person5	0	1	1	5	78	5	0	0.867	0.952	0.133	93.2
Person6	0	8	1	6	4	41	0	0.683	0.959	0.317	91.7
Person7	4	0	4	2	3	0	17	0.567	0.980	0.433	94.8
Naive Bayes	Person1	Person2	Person3	Person4	Person5	Person6	Person7	Sensitivity	Specificity	FAR	ACC
Person1	53	0	0	0	3	0	4	0.883	0.984	0.117	96.9
Person2	0	20	0	4	0	3	3	0.667	0.991	0.433	96.6
Person3	0	0	49	0	0	8	3	0.817	0.984	0.183	95.8
Person4	5	1	0	21	12	0	15	0.389	0.936	0.611	85.9
Person5	0	0	0	10	75	2	3	0.833	0.918	0.167	89.8
Person6	0	2	2	5	6	45	0	0.75	0.959	0.25	92.7
Person7	0	0	3	2	3	0	22	0.733	0.92	0.267	90.6
Decision Tree	Person1	Person2	Person3	Person4	Person5	Person6	Person7	Sensitivity	Specificity	FAR	ACC
Person1	51	0	0	4	0	0	5	0.85	0.966	0.15	94.8
Person2	0	20	0	5	0	5	0	0.667	0.954	0.333	93.2
Person3	0	0	55	0	0	2	3	0.917	0.984	0.083	97.4
Person4	5	7	1	21	9	8	3	0.389	0.939	0.611	86.2
Person5	1	0	0	6	81	2	0	0.9	0.942	0.1	93.2
Person6	0	7	2	3	7	41	0	0.683	0.947	0.317	90.6
Person7	5	2	2	2	1	0	18	0.6	0.968	0.4	94
SVM	Person1	Person2	Person3	Person4	Person5	Person6	Person7	Sensitivity	Specificity	FAR	ACC
Person1	58	0	0	1	0	0	1	0.967	0.947	0.033	95.1
Person2	1	13	0	5	0	8	3	0.433	0.983	0.567	94
Person3	1	1	53	1	0	2	2	0.883	0.996	0.117	97.9
Person4	11	0	0	19	14	0	10	0.352	0.948	0.648	86.5
Person5	0	0	0	6	84	0	0	0.933	0.908	0.067	91.4
Person6	0	5	0	3	8	44	0	0.733	0.969	0.267	93.2
Person7	4	0	1	1	5	0	19	0.633	0.954	0.367	93

Table 7 –Rotation task results.

NN	Person1	Person2	Person3	Person4	Person5	Person6	Person7	Sensitivity	Specificity	FAR	ACC
Person1	52	0	1	6	1	0	0	0.867	0.981	0.133	96.4
Person2	0	19	5	1	1	4	0	0.633	0.963	0.367	93.8
Person3	0	5	49	0	3	0	3	0.817	0.96	0.183	93.8
Person4	3	0	2	38	14	2	1	0.633	0.957	0.367	90.8
Person5	2	0	1	5	78	4	0	0.867	0.926	0.133	91.3
Person6	0	8	1	2	3	46	0	0.767	0.969	0.233	93.8
Person7	1	0	3	0	0	0	26	0.867	0.988	0.133	97.9
Naive Bayes	Person1	Person2	Person3	Person4	Person5	Person6	Person7	Sensitivity	Specificity	FAR	ACC
Person1	54	0	0	6	0	0	0	0.9	0.969	0.1	95.9
Person2	0	25	2	0	0	3	0	0.833	0.972	0.167	96.2
Person3	0	6	46	3	1	2	2	0.767	0.975	0.233	94.4
Person4	7	1	5	33	13	0	1	0.55	0.921	0.45	86.4
Person5	3	0	0	10	77	0	0	0.856	0.953	0.144	93.1
Person6	0	3	0	7	0	50	0	0.833	0.984	0.167	96.2
Person7	0	0	1	0	0	0	29	0.967	0.991	0.033	99
Decision Tree	Person1	Person2	Person3	Person4	Person5	Person6	Person7	Sensitivity	Specificity	FAR	ACC
Person1	51	0	0	8	1	0	0	0.85	0.975	0.15	95.6
Person2	0	16	2	1	2	9	0	0.533	0.952	0.467	92.1
Person3	0	3	50	3	1	0	3	0.833	0.966	0.167	94.6
Person4	8	2	5	33	11	1	0	0.55	0.936	0.45	87.7
Person5	0	4	0	9	77	0	0	0.856	0.946	0.144	92.6
Person6	0	8	0	0	0	52	0	0.867	0.969	0.133	95.4
Person7	0	0	4	0	1	0	25	0.833	0.991	0.167	97.9
SVM	Person1	Person2	Person3	Person4	Person5	Person6	Person7	Sensitivity	Specificity	FAR	ACC
Person1	53	0	0	3	4	0	0	0.883	0.981	0.117	96.7
Person2	0	15	4	2	0	8	1	0.5	0.98	0.5	94.4
Person3	0	2	56	0	0	1	1	0.933	0.972	0.067	96.7
Person4	1	2	0	38	15	0	4	0.633	0.96	0.367	91
Person5	3	0	0	4	83	0	0	0.922	0.93	0.078	92.8
Person6	0	3	1	4	2	50	0	0.833	0.972	0.167	95.1
Person7	2	0	4	0	0	0	24	0.8	0.983	0.2	96.9

Table 8 –Counting task results.

NN	Person1	Person2	Person3	Person4	Person5	Person6	Person7	Sensitivity	Specificity	FAR	ACC
Person1	50	0	0	9	1	0	0	0.833	0.942	0.167	92.6
Person2	0	25	3	0	1	1	0	0.833	0.98	0.167	96.9
Person3	0	5	52	0	0	1	2	0.867	0.99	0.133	97.2
Person4	19	0	0	33	6	0	2	0.55	0.957	0.45	89.5
Person5	0	0	0	5	85	0	0	0.944	0.97	0.056	96.4
Person6	0	2	0	0	1	57	0	0.95	0.993	0.05	98.7
Person7	0	0	0	0	0	0	30	1	0.988	0	99
Naïve Bayes	Person1	Person2	Person3	Person4	Person5	Person6	Person7	Sensitivity	Specificity	FAR	ACC
Person1	48	0	0	9	2	0	1	0.8	0.93	0.2	91
Person2	0	28	0	0	2	0	0	0.933	0.963	0.067	96.2
Person3	0	9	51	0	0	0	0	0.85	0.99	0.15	96.9
Person4	22	0	0	34	4	0	0	0.567	0.921	0.433	86.7
Person5	0	0	1	16	73	0	0	0.811	0.956	0.189	92.3
Person6	0	4	2	0	5	49	0	0.817	1	0.183	97.2
Person7	1	0	0	1	0	0	28	0.933	0.997	0.067	99.2
Decision Tree	Person1	Person2	Person3	Person4	Person5	Person6	Person7	Sensitivity	Specificity	FAR	ACC
Person1	42	0	0	14	2	0	2	0.7	0.954	0.3	91.5
Person2	0	18	4	1	2	5	0	0.6	0.972	0.4	94.4
Person3	0	3	52	0	3	2	0	0.867	0.978	0.133	96.2
Person4	14	0	0	41	5	0	0	0.683	0.933	0.317	89.5
Person5	0	1	1	7	81	0	0	0.9	0.956	0.1	94.4
Person6	0	5	1	0	1	53	0	0.883	0.978	0.117	96.4
Person7	1	1	1	0	0	0	27	0.9	0.994	0.1	98.7
SVM	Person1	Person2	Person3	Person4	Person5	Person6	Person7	Sensitivity	Specificity	FAR	ACC
Person1	43	0	0	14	2	0	1	0.717	0.942	0.283	90.8
Person2	0	23	0	0	2	5	0	0.767	0.969	0.233	95.4
Person3	0	8	51	0	0	0	1	0.85	0.987	0.15	96.7
Person4	19	0	0	33	6	0	2	0.55	0.948	0.45	88.7
Person5	0	0	0	3	87	0	0	0.967	0.95	0.037	95.4
Person6	0	3	4	0	5	48	0	0.8	0.984	0.2	95.6
Person7	0	0	0	0	0	0	30	1	0.988	0	99

Table 9 –Counting task results per features.

NN	Sensitivity	Specificity	FAR	ACC
EEG_Mean	0.329	0.889	0.67	35.38
EEG_Std	0.839	0.973	0.16	84.61
EEG_Entropy	0.691	0.95	0.308	70.76
EEG_Energy	0.329	0.889	0.67	35.38

Acknowledgement

This research has been done under USM Grant (1001/PKOMP/8014016). Also, the first author would like to thank The World Academic Science (TWAS) and the University Science Malaysia (USM) for supporting his study (TWAS-USM Postgraduate Fellowship 2015, FR number: 3240287134).

References

- [1] Abdi, Z., Alyasseri, A., Khader, A. T., Al-betar, M. A., Awadallah, M. A., & Yang, X. (2018). Variants of the Flower Pollination Algorithm : A Review. https://doi.org/10.1007/978-3-319-67669-2_5
- [2] Abdulkader, S. N., Atia, A., & Mostafa, M. S. M. (2015). Brain computer interfacing: Applications and challenges. *Egyptian Informatics Journal*, 16(2), 213–230. <https://doi.org/10.1016/j.eij.2015.06.002>
- [3] Abo-Zahhad, M., Ahmed, S. M., & Abbas, S. N. (2016). A new multi-level approach to EEG based human authentication using eye blinking. *Pattern Recognition Letters*, 82, 216–225. <https://doi.org/10.1016/j.patrec.2015.07.034>
- [4] Abualigah, L. M., Khader, A. T., Al-Betar, M. A., Alyasseri, Z. A. A., Alomari, O. A., & Hanandeh, E. S. (2017). Feature Selection with β -Hill Climbing Search for Text Clustering Application. In *Proceedings - 2017 Palestinian International Conference on Information and Communication Technology, PICICT 2017*. <https://doi.org/10.1109/PICICT.2017.30>
- [5] Al-betar, M. A. (2017). -Hill climbing: an exploratory local search. *Neural Computing and Applications*. <https://doi.org/10.1007/s00521-016-2328-2>
- [6] Al-Betar, M. A., Alyasseri, Z. A. A., Khader, A. T., La 'aro Bolaji, A., & Awadallah, M. A. (2016). Gray image enhancement using harmony search. *International Journal of Computational Intelligence Systems*, 9(5), 932–944.
- [7] Alyasseri, Z. A. A., Khader, A. T., & Al-Betar, M. A. (2017). Electroencephalogram Signals Denoising using Various Mother Wavelet Functions: A Comparative Analysis. *Proceedings of the International Conference on Imaging, Signal Processing and Communication*, 100–105. <https://doi.org/10.1145/3132300.3132313>
- [8] Alyasseri, Z. A. A., Khader, A. T., & Al-Betar, M. A. (2017). Optimal electroencephalogram signals denoising using hybrid β -hill climbing algorithm and wavelet transform. In *ACM International Conference Proceeding Series (Vol. Part F1313)*. <https://doi.org/10.1145/3132300.3132314>
- [9] Alyasseri, Z. A. A., Khader, A. T., Al-Betar, M. A., & Abualigah, L. M. (2017). ECG signal denoising using β -hill climbing algorithm and wavelet transform. *ICIT 2017 The 8th International Conference on Information Technology*.
- [10] Alyasseri, Z. A. A., Khader, A. T., Al-Betar, M. A., & Awadallah, M. A. (2018). Hybridizing β -hill climbing with wavelet transform for denoising ECG signals. *Information Sciences*, 429. <https://doi.org/10.1016/j.ins.2017.11.026>
- [11] Alyasseri, Z. A. A., Venkat, I., Al-Betar, M. A., & Khader, A. T. (2012). Edge preserving image enhancement via harmony search algorithm. In *Conference on Data Mining and Optimization*. <https://doi.org/10.1109/DMO.2012.6329797>
- [12] Alyasseri, Z. A. A., Khader, A. T., Al-Betar, M. A., Papa, J. P., & ahmad Alomari, O. (2018, July). EEG-based Person Authentication Using Multi-objective Flower Pollination Algorithm. In *2018 IEEE Congress on Evolutionary Computation (CEC)* (pp. 1-8). IEEE.
- [13] Berger, H. (1929). Uber das Elektrenkephalogramm des Menschen (On the human elec- troencephalogram). *Archiv f. Psychiatrie u. Nervenkrankheiten*, 87(1875), 527–570. <https://doi.org/10.1007/BF01797193>
- [14] Donoho, D. L., & Johnstone, I. M. (1994). Ideal spatial adpatation by wavelet shrinkage. *Biometrika*, 81, 425–455.
- [15] Keirn, Z. A., & Aunon, J. I. (1990). A New Mode of Communication Between Man and his Surroundings. *IEEE Transactions on Biomedical Engineering*, 37(12), 1209–1214. <https://doi.org/10.1109/10.64464>
- [16] Kumari, P., & Vaish, A. (2015). Brainwave based user identification system: A pilot study in robotics environment. *Robotics and Autonomous Systems*, 65, 15–23. <https://doi.org/10.1016/j.robot.2014.11.015>
- [17] Kumari, P., & Vaish, A. (2016). Feature-level fusion of mental task's brain signal for an efficient identification system. *Neural Computing and Applications*, 27(3), 659–669. <https://doi.org/10.1007/s00521-015-1885-0>
- [18] Kumari Sharma, P., & Vaish, A. (2016). Individual identification based on neuro-signal using motor movement and imaginary cognitive process. *Optik*, 127(4), 2143–2148. <https://doi.org/10.1016/j.ijleo.2015.09.020>
- [19] Ramadan, R. A., & Vasilakos, A. V. (2017). Brain computer interface: control signals review. *Neurocomputing*, 223(August), 26–44. <https://doi.org/10.1016/j.neucom.2016.10.024>
- [20] Rao, R. P. N. (2013). Brain-computer interfacing: An introduction. *Brain-Computer Interfacing: An Introduction*. <https://doi.org/10.1017/CBO9781139032803>
- [21] Rodrigues, D., Silva, G. F. A., Papa, J. P., Marana, A. N., & Yang, X. S. (2016). EEG-based person identification through Binary Flower Pollination Algorithm. *Expert Systems with Applications*, 62, 81–90. <https://doi.org/10.1016/j.eswa.2016.06.006>
- [22] Sarier, N. D. (2010). Improving the accuracy and storage cost in biometric remote authentication schemes. *Journal of Network and Computer Applications*, 33(3), 268–274. <https://doi.org/10.1016/j.jnca.2009.12.017>
- [23] Schalk, G., McFarland, D. J., Hinterberger, T., Birbaumer, N., & Wolpaw, J. R. (2004). BCI2000: A General-Purpose Brain-Computer Interface (BCI) System. *IEEE Transactions on Biomedical Engineering*, 51(6), 1034–1043. <https://doi.org/10.1109/TBME.2004.827072>
- [24] Yang, X.-S. (2013). Flower Pollination Algorithm for Global Optimization. https://doi.org/10.1007/978-3-642-32894-7_27
- [25] Yang, X. S., Karamanoglu, M., & He, X. (2014). Flower pollination algorithm: A novel approach for multiobjective optimization. *Engineering Optimization*, 46(9), 1222–1237. <https://doi.org/10.1080/0305215X.2013.832237>